International Journal of Research in Engineering and Science (IJRES)
ISSN (Online): 2320-9364, ISSN (Print): 2320-9356
www.ijres.org Volume 11 Issue 10 ǁ October 2023 ǁ PP. 341-350

Study of Joule Effect of Aluminium Oxide nanofluid using Cattaneo-Christov over a Cylinder

Zaffer Elahi∗,Azra Faiz†,Azeem Shahzad‡

Abstract *The objective of this article is to study the effect of Joule heating on heat transfer in the Cattaneo-Christov model on a cylinder that is being stretched. The investigation specifically focuses on the influence of various shapes of aluminium oxide nanoparticles dispersed in ethylene glycol (EG) on the heat transfer characteristics. The governing partial differential equations (PDEs) that describe the heat transfer process are transformed into ordinary differential equations (ODEs) using suitable transformations. The resulting ODEs are then solved numerically utilizing the BVP4C method implemented in MATLAB. The study examines the impact of different physical parameters on the temperature profile are presented graphically. Furthermore, the skin friction coefficient and Nusselt number are calculated in tables.*
Keywords: *Aluminium Oxide nanofluid; Cattaneo-Christov Model; Joule Effect.*

Date of Submission: 14-10-2023 Date of acceptance: 29-10-2023

Keywords: Aluminium Oxide nanofluid; Cattaneo-Christov Model; Joule Effect.|

Nomenclature:

T_∞	Slit temperature (K)
κ_f	Thermal conductivity of base fluid $(W/K/m)$
κ_{nf}	Thermal conductivity of nanofluid $(W/K/m)$
C_p	Specific heat of fluid $(J/kg/K)$
C_f	Skin friction coefficient (-)
α_f	Thermal diffusion of base fluid (m^2/s)
α_{nf}	Thermal diffusivity of nanofluid (m^2/s)
ρ_f	Density of base fluid (water) (kg/m^3)
ρ_{nf}	Density of nanofluid (kg/m^3)
μ_f	Dynamic viscosity of base fluid $(kg\ m/s)$
μ_{nf}	Dynamic viscosity of nanofluid $(kg\ m/s)$
σ_{nf}	Electrical conductivity of nanofluid (-)
$(\rho C_p)_{nf}$	Heat capacity of nanofluid (-)

∗zaffer.elahi@uettaxila.edu.pk, Department of Basic Sciences, University of Engineering and Technology, Taxila -47050, Pakistan,
†azrafaiz243@gmail.com, Department of Basic Sciences, University of Engineering and Technology, Taxila -47050, Pakistan,
‡azeem.shahzad@uettaxila.edu.pk, Department of Basic Sciences, University of Engineering and Technology, Taxila -47050, Pakistan.

I. Introduction

In recent years, the use of nanofluids and advanced mathematical models has gained significant attention in the field of heat transfer and fluid mechanics. The Cattaneo-Christov model and nanofluids have been subjects of extensive research. One of the most promising applications of nanotechnology is the production of high thermal conductivity nanoparticles that can be mixed with base fluids to form nanofluids. Nanofluids containing particles between (1-100) nm such as, copper, alumina, carbides, silica, nitride, metal oxides, graphite, and carbon nanotubes are used to enhance the thermal conductivity of base fluids like water, engine oils, glycerol, and ethylene glycol. Nanofluids have a wide range of applications in industry, including heating and cooling systems, solar cells, the generation of new fuels, hybrid-powered engines, biomedical applications, cancer therapy, and drug delivery [1-2]. In contrast, Fourier's law, which is a fundamental mathematical relation of heat conduction, leads to a parabolic-type equation for the temperature field that means heat transfer has infinite speed and propagates throughout the medium with an initial disturbance [3]. To overcome this limitation, Cattaneo modified Fourier's law by introducing the thermal relaxation time parameter, which multiplies with the time derivative of heat flux, yielding a hyperbolic-type equation for heat transport, and as a result, the transport of heat has a finite speed in the entire medium. The Cattaneo- Christov model is a modified form of the classical Fourier's law of

heat conduction. A brief review of existing literature regarding the Cattano-Christov model over a stretching cylinder is given. Ibrahim et. al. [4] Studied finite element solution of nonlinear convective flow of Oldroyd-B fluid with Cattaneo-Christov heat flux model over nonlinear stretching surface with heat generation or absorption. Ganesh et. al. [5] studied hydromagnetics axisymmetric slip flow along a vertical stretching cylinder with convective boundary condition. Makinde et. al. [6] analyzed the effects of Cattaneo-Christov heat flux on Casson nanofluid flow past a stretching cylinder. Babu et. al. [7] studied thermal radiation impact and Cattaneo-christov theory for the unsteady flow of maxwell fluid over the stretched cylinder with inconsistent heat source/sink. Tulu et. al. [8] investigated the MHD slip flow of CNT-ethylene glycol nanofluid due to a stretchable rotating disk with the Cattaneo–Christov heat flux model. Elahi et. al. [9] investigated the effect of the Cattaneo-Christov model over a vertical stretching cylinder using SiO2 nanofluid. Khan et. al. [10] analyzed the effect of the Cattaneo-Christov theory on unsteady the flow of Maxwell fluid over a stretching cylinder. Additionally, considering the Joule heating effect on heat transfer in nanofluids flowing along a stretching cylinder enables a deeper understanding of the interaction between electrical energy and thermal energy. This understanding can lead to more accurate predictions of heat transfer performance and inform the design of efficient nanofluid-based systems. Wang et. al. [11] studied the Joule heating effect in nanofluids heat and Mass transfer. Vanaki et. al. [12] investigated the Joule heating effect and heat transfer in MHD nanofluids flow over a stretching sheet by means of CVFEM. Rahimi et. al. [13] investigated the numerical simulation of nanofluid flow and heat transfer over a stretching cylinder considering the Joule heating effect. Using the Cattaneo-Christov model in an unsteady situation, this work aims to investigate the effect of Joule heating of aluminium oxide nanofluid over a cylinder in the light of earlier studies.

II. Development of Physical Model and Problem Formulation

Consider the fluid flow across a stretching cylinder with a Joule heating coefficient in the Cattaneo-Christov model, which is two-dimensional and incompressible. Assume that the fluid is moving due to the stretching of the cylinder at velocity $U_w(z) = \frac{cz}{1-\alpha t}$ in the z-direction and $T_w = T_\infty + \frac{cz}{(1-\alpha t)^2}$ is the temperature of the surface where c and α are dimensional constants. In the r-direction, the uniform magnetic field B_0 acts perpendicularly, as shown in Figure 1.

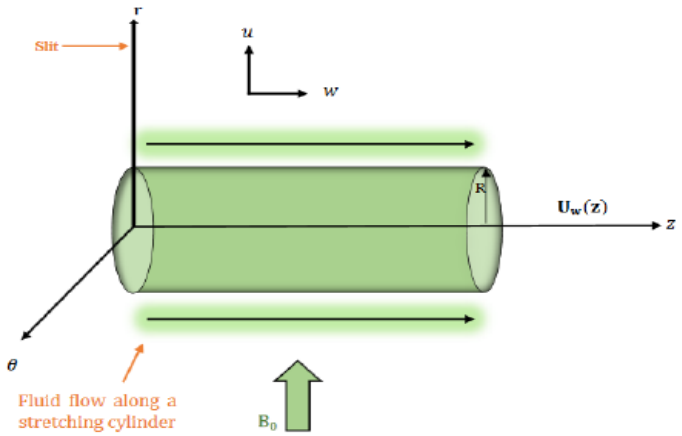

Figure 1: Geometrical Representation of the Proposed Model

Let $u(r,z,t)$ and $w(r,z,t)$ represent the velocity components in the r- and z-directions, respectively, and $T(r,z,t)$ denote the temperature of the fluid. Under the assumption of a boundary layer approximation, the governing equations can be obtained, as

$$\frac{\partial(ru)}{\partial r} + \frac{\partial(rw)}{\partial z} = 0, \tag{1}$$

$$\frac{\partial w}{\partial t} + u\frac{\partial w}{\partial r} + w\frac{\partial w}{\partial z} = \frac{\mu_{nf}}{\rho_{nf}}\left[\frac{1}{r}\frac{\partial}{\partial r}\left(r\frac{\partial w}{\partial r}\right)\right] - \frac{\sigma_{nf}}{\rho_{nf}}B_0^2 w \tag{2}$$

$$\rho_{nf}c_p\left(\frac{\partial T}{\partial t} + u\frac{\partial T}{\partial r} + w\frac{\partial T}{\partial z}\right) = -\nabla\cdot q + \mu_{nf}\left(\frac{\partial w}{\partial r}\right)^2 + \frac{J^2}{\sigma_{nf}}. \tag{3}$$

The heat flux equation, according to Han *et* al. [14], must satisfy the following relation. Using the heat flux equation in (3) we get equation (4) as,

$$\frac{\partial T}{\partial t}+u\frac{\partial T}{\partial r}+w\frac{\partial T}{\partial z}=\frac{\mu_{nf}}{\rho_{nf}c_p}\left(\frac{\partial w}{\partial r}\right)^2+\frac{\alpha_{nf}}{r}\frac{\partial}{\partial r}\left(r\frac{\partial T}{\partial r}\right)+\lambda_1\left[\frac{2\mu_{nf}}{\rho_{nf}c_p}\frac{\partial w}{\partial r}\right.$$

$$\left(\frac{\partial^2 w}{\partial t\partial r}+u\frac{\partial^2 w}{\partial r^2}+w\frac{\partial^2 w}{\partial z\partial r}\right)+2\frac{\sigma_{nf}}{\rho_{nf}c_p}B_0^2 w\left(\frac{\partial w}{\partial t}+u\frac{\partial w}{\partial r}+w\frac{\partial w}{\partial z}\right)-$$

$$\left\{\left(\frac{\partial^2 T}{\partial t^2}+u^2\frac{\partial^2 T}{\partial r^2}+w^2\frac{\partial^2 T}{\partial z^2}+2uw\frac{\partial^2 T}{\partial z\partial r}+2u\frac{\partial^2 T}{\partial r\partial t}+2w\frac{\partial^2 T}{\partial t\partial z}\right)\right.$$

$$\left.\left.+\frac{\partial T}{\partial r}\left(\frac{\partial u}{\partial t}+u\frac{\partial u}{\partial r}+w\frac{\partial u}{\partial z}\right)+\left(\frac{\partial w}{\partial t}+u\frac{\partial w}{\partial r}+w\frac{\partial w}{\partial z}\right)\frac{\partial T}{\partial z}\right)\right\}\Bigg]+\frac{\sigma_{nf}}{\rho_{nf}c_p}B_0^2 w^2, \tag{4}$$

subject to the boundary conditions

$$\left.\begin{aligned} u=0,\quad w=U_w,\quad \frac{\partial T}{\partial r}=0\quad at\quad r=R,\\ w\to 0,\quad T\to T_\infty\quad as\quad r\to\infty,\end{aligned}\right\} \tag{5}$$

The thermophysical properties of nanofluids [15, 16] are

$$\alpha_{nf}=\frac{\kappa_{nf}}{(\rho C_p)_{nf}},\qquad \rho_{nf}=(1-\phi)\rho_f+\phi\rho_s,$$

$$\mu_{nf}=\mu_f(1+A_1\phi+A_2\phi^2),\qquad \sigma_{nf}=\sigma_f(1-\phi)\sigma_f+\phi\sigma_s,$$

$$(\rho C_p)_{nf}=(1-\phi)(\rho C_p)_f+\phi(\rho C_p)_s,\qquad \frac{\kappa_{nf}}{\kappa_f}=\left[\frac{\kappa_s+(m-1)\kappa_f+(m-1)(\kappa_s-\kappa_f)\phi}{\kappa_s+(m-1)\kappa_f-(\kappa_s-\kappa_f)\phi}\right]. \tag{6}$$

Here to make the system dimensionless we introduce the following transformations [17,18]

$$\theta(\eta)=\frac{T-T_\infty}{T_\omega-T_\infty},\qquad \eta=\left(\frac{c}{\nu_f(1-\alpha t)}\right)^{\frac{1}{2}}\left(\frac{r^2-R^2}{2R}\right),\qquad \psi=\left(\frac{c\nu_f}{1-\alpha t}\right)^{\frac{1}{2}}zRf(\eta), \tag{7}$$

where the flow pattern ψ is defined as

$$u=-\frac{1}{r}\frac{\partial\psi}{\partial z},\qquad and\qquad w=\frac{1}{r}\frac{\partial\psi}{\partial r}$$

that satisfies the continuity equation (1) directly.

The momentum equation (2) and energy equation (4) with boundary condition (5) lead to (8-10).

$$\epsilon_1(1+2\kappa\eta)f'''(\eta)+2\epsilon_1\kappa f''(\eta)+\left[f(\eta)f''(\eta)-f'^2(\eta)-S\left(f'(\eta)+\frac{\eta}{2}f''(\eta)\right)\right]-\epsilon_3 M f'(\eta)=0, \tag{8}$$

$$\epsilon_1(1+2\kappa\eta)E_c f'^2(\eta)+\frac{\epsilon_1}{P_r}\left(2\kappa\theta'(\eta)+(1+2k\eta)\theta''(\eta)\right)+\beta_1\left[(1+2\kappa\eta)\left(3\epsilon_1 sE_c f'^2(\eta)+\right.\right.$$

$$\left.\eta sE_c 3f''(\eta)f'''(\eta)-2E_c f(\eta)f''(\eta)f'''(\eta)+E_c f'(\eta)f''(\eta)\right)+2\epsilon_3 E_c M\left(s(f'^2(\eta)+\frac{\eta}{2}f'(\eta)f''(\eta))-\right.$$

$$f(\eta)f'(\eta)f''(\eta)+f'^3(\eta)\Big)-s^2\left(6\theta(\eta)+\frac{11}{4}\eta\theta'(\eta)+\frac{\eta^2}{4}\theta''(\eta)\right)-\frac{s}{2}\left(10f'(\eta)\theta(\eta)-11f(\eta)\theta'(\eta)\right.$$

$$\left.+\eta f'(\eta)\theta'(\eta)+\eta f''(\eta)\theta(\eta)-2\eta f(\eta)\theta''(\eta)\right)+f(\eta)f''(\eta)\theta(\eta)-f'^2(\eta)\theta(\eta)-2\kappa E_c f(\eta)f'^2(\eta)-$$

$$\left.f^2(\eta)\theta''(\eta)+f(\eta)f'(\eta)\theta'(\eta)\right]-s\left(2\theta(\eta)+\frac{\eta}{2}\theta'(\eta)\right)+f(\eta)\theta'(\eta)-f'(\eta)\theta(\eta)+\epsilon_3 E_c M f'^2(\eta)=0, \tag{9}$$

$$f(\eta) = 0, \quad f'(\eta) - 1 = 0, \quad \theta(\eta) - 1 = 0 \quad at \quad \eta = 0,$$
$$f'(\eta) \to 0, \quad \theta(\eta) \to 0 \quad as \quad \eta \to \infty. \tag{10}$$

The constants $\epsilon_i,\ i = 1, \ldots, 3$ are used in (8) and (9), defined as

$$\epsilon_1 = \frac{1 + A_1\phi + A_2\phi^2}{1 - \phi + \phi\left(\frac{\rho_s}{\rho_f}\right)}, \quad \epsilon_2 = \frac{\left(\frac{\kappa_{nf}}{\kappa_f}\right)}{1 - \phi + \phi\frac{(\rho C_p)_s}{(\rho C_p)_f}}, \quad \epsilon_3 = \frac{1 - \phi + \phi\left(\frac{\sigma_s}{\sigma_f}\right)}{1 - \phi + \phi\left(\frac{\rho_s}{\rho_f}\right)}, \tag{11}$$

where ϕ is the solid volume fraction parameter.

Moreover, we have the following significant non-dimensional physical parameters in these equations,

$$\kappa = \frac{1}{R}\left(\frac{\nu_f(1-\alpha t)}{c}\right)^{\frac{1}{2}}, \qquad Ec = \frac{U_w^2}{C_p(T_w - T)}, \qquad M = \frac{\beta_0\sigma_f(1-\alpha t)}{c\rho_{nf}},$$
$$Pr = \frac{(\rho\ C_p)_f\ \nu_f}{\kappa_f}, \qquad S = \frac{\alpha}{c}, \qquad \beta_1 = \frac{c\lambda_1}{1-\alpha t}$$

Since the rate of shear stress and strain at the surface of a horizontally stretched cylinder can be defined, as

$$C_f = \frac{2\tau_w}{\rho_f\ U_w^2} = \frac{2\mu_{nf}}{\rho_f\ U_w^2}\left[\frac{\partial u}{\partial r}\right]_{r=R}, \tag{12}$$

and

$$Nu = \frac{zq_w}{\kappa_f\ (T_w - T_\infty)} = -\frac{z\kappa_{nf}}{\kappa_f\ (T_w - T_\infty)}\left[\frac{\partial T}{\partial r}\right]_{r=R}. \tag{13}$$

In non-dimensional form (12) and (13) can be written, as

$$\frac{1}{2}Re^{\frac{1}{2}}C_f = (1 + A_1\phi + A_2\phi^2)\ f''(0) \quad and \quad Re^{-\frac{1}{2}}Nu = -\frac{\kappa_{nf}}{\kappa_f}\ \theta'(0). \tag{14}$$

The thermophysical properties of the Ethylene Glycol (EG) and the suspended particles' viscosity and shape of the particles are defined in Table 1-2.

Table 1: Thermophysical properties of EG and Aluminium Oxide nanofluid [19,20,21,22]

Nanoparticle/ Base fluid	(kg/m^3)	$(W/m\,K)$	$(J/kg\,K)$	(S/m)
Aluminium Oxide	3970	40	765	35×10^{-6}
Ethylene Glycol	1115	0.253	2430	3.14×10^{6}

Table 2: Viscosity and shape factor of nanoparticles [23, 24, 25]

Parameters/ Nanoparticles	A_1	A_2	**m**
Sphere	2.5	6.5	3.0
Blade	14.6	123.3	8.26

III. Method of Solution

To numerically solve the nonlinear system (8-10), the system is transformed into a set of first-order linear equations, considering the following considerations.

$$\left.\begin{aligned} f &= y_1, \\ y_1' &= y_2, \\ y_2' &= y_3, \\ y_3' &= g_1, \\ y_4 &= \theta, \\ y_4' &= y_5, \\ y_5' &= g_2, \end{aligned}\right\} \tag{15}$$

where

$$g_1 = \frac{1}{\epsilon_1(1+2\eta\kappa)}\left[\epsilon_3\, M y_2 - 2\epsilon_1\kappa y_3 - \left\{y_1 y_3 - y_2^2 - S\left(y_2 + \frac{\eta}{2}y_3\right)\right\}\right], \tag{16}$$

and

$$g_2 = \frac{4Pr}{4(1+2\kappa\eta)\epsilon_1 - Pr\beta_1\left(S^2\eta^2 - 4S\eta\, y_1 + 4y_1^2\right)}\left[S\left(2y_4 + \frac{\eta}{2}y_5\right) - y_1 y_5 + y_2 y_4 - \left(\frac{2\epsilon_1\kappa y_5}{Pr}\right)\right.$$

$$-(1+2\kappa\eta)\epsilon_1 Ec\, y_3^2 - \epsilon_3 E_c M y_2^2 - \beta_1\left\{\epsilon_1 Ec(1+2\kappa\eta)\left(3Sy_3^2 + 2y_2y_3 + S\eta y_3 y_3' - 2y_1y_3y_3'\right)\right.$$

$$-\frac{S^2}{4}\left(24y_4 + 11\eta y_5\right) + \frac{S}{2}\left\{10y_2y_4 - 11y_1y_5 + \eta y_2y_5 + \eta\, y_3y_4\right\} - 2\epsilon_1 E_c\kappa y_1 y_3^2 + 2\epsilon_3 E_c M$$

$$\left.\left.\left(sy_2^2 + s\frac{\eta}{2}y_2y_3 - y_1y_2y_3 + y_2^3\right) + y_1y_2y_5 + y_1y_3y_4 - y_2^2y_4\right\}\right]. \tag{17}$$

The boundary conditions are

$$y_1(\eta) = 0, \qquad y_2(\eta) = 1, \qquad y_4(\eta) - 1 = 0 \quad at \quad \eta = 0,$$

$$y_2(\eta) \to 0, \qquad y_4(\eta) \to 0 \quad at \quad \eta \to \infty. \tag{18}$$

Solving the system of first-order equations (15-17) together with (18) using BVP4C packages Matlab. The result is presented graphically and in tabular form in the following section.

IV. Results and Discussion

We will present a brief analysis of the numerical investigation of heat transfer of aluminium oxide, considering the Joule effect in the Cattaneo-Christov model for different nanoparticle shapes (Sphere and Blade) in this section. We will also study the impact of nanoparticle shapes and different parameters on temperature distribution graphically. Also, the skin friction and the Nusselt number have been computed for different parameters.

Figure 2 shows the effect of the thermal relaxation time parameter (β_1). The temperature field is increased by continuously varying the β_1 values. Figure 3 shows the impact of Eckert number (Ec) on the temperature profile. The temperature profile increases for the higher values of Ec. Figure 4 demonstrates the effect of the magnetic parameter (M) on the temperature profile which shows the temperature dimensionless increases with increasing magnetic field. Figure 5 is plotted to examine the influence of the Prandtl number (Pr) on temperature. It is clear from the graphical trend that the temperature profile reflects an inverse nature towards the higher values of Pr. Figure 6 depicts the effect of volume-fraction (ϕ) on the temperature profile. It shows the temperature profile for each shape of nanoparticle is increased for the increasing values of ϕ. Figure 7 shows the effect of the unsteadiness parameter (S) on temperature distribution. The temperature profile decreases for increasing values of S.

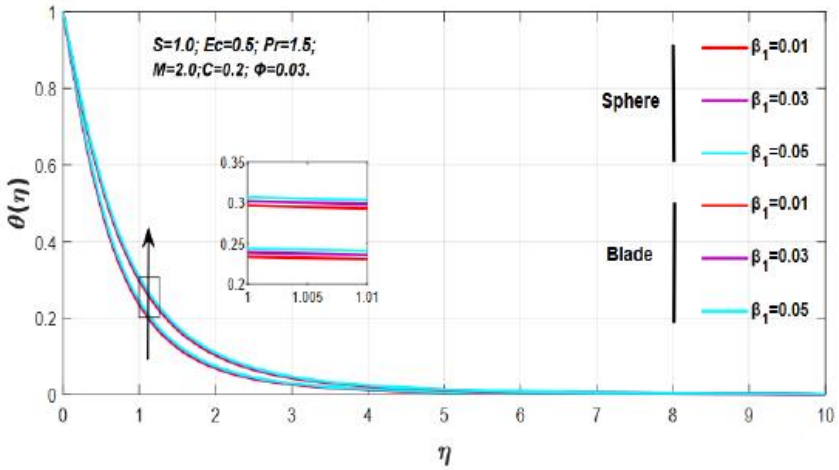

Figure 2: Effect of Thermal relaxation time parameter (β_1) on temperature profile

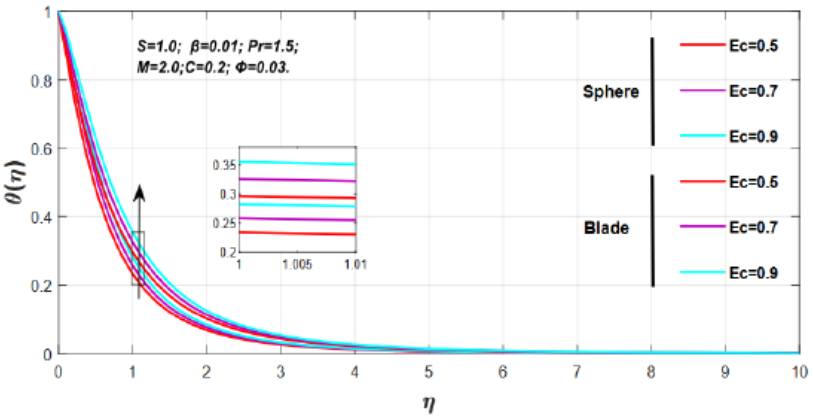

Figure 3: Effect of Eckert number (Ec) on temperature profile

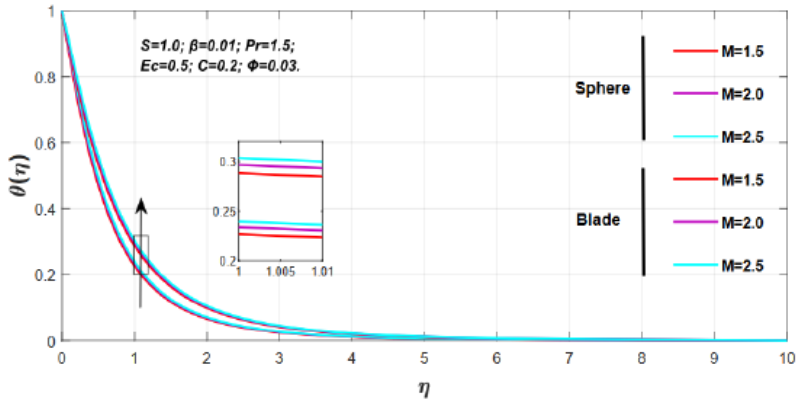

Figure 4: Effect of Magnetic parameter (M) on temperature profile

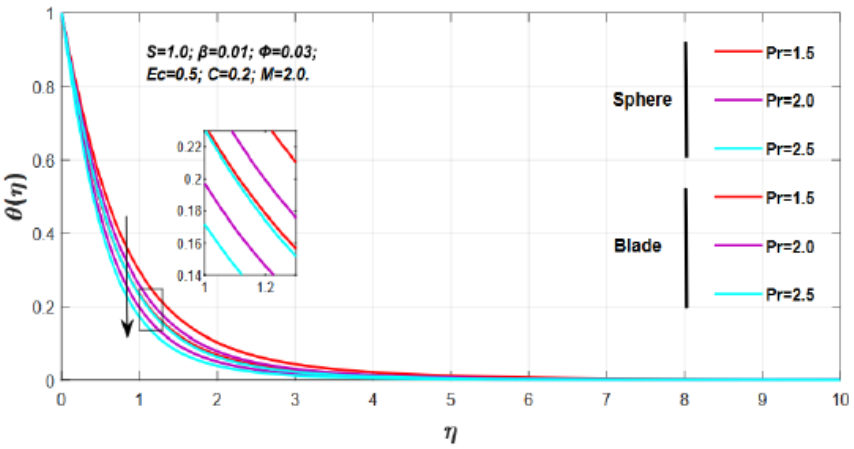

Figure 5: Effect of Prandtl number (Pr) on temperature profile

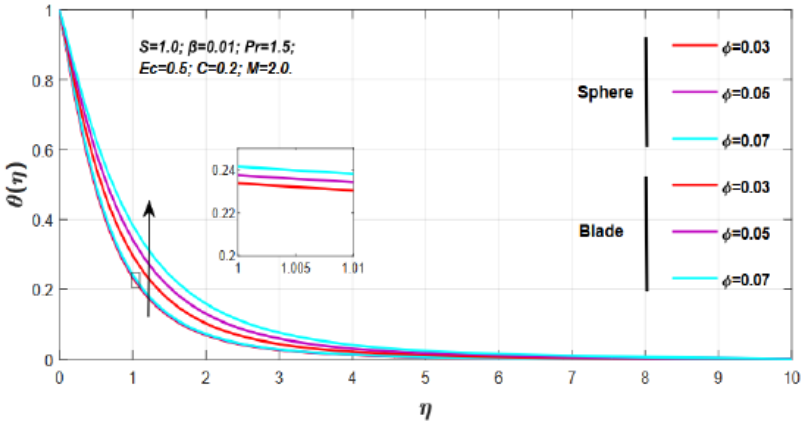

Figure 6: Effect of Volume fraction (ϕ) on temperature profile

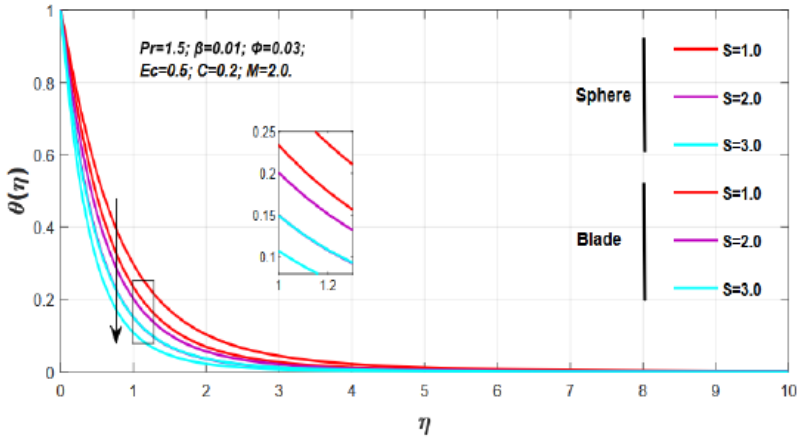

Figure 7: Effect of Unsteadiness parameter (S) on temperature profile

It is observed that the temperature profile increases for the growing values of the (β_1), (Ec), (M), and (ϕ). On the other hand, the temperature profile decreases for the increasing values of (Pr) and (S).

The skin friction and nusselt coefficients have been computed, for each shape of nanoparticles by varying the physical parameters numerically in Table 3-4 respectively.
In Table 3, it is observed the increase in volume-fraction ϕ, magnetic field M, and unsteadiness parameter S for each shape of nanoparticles.

Table 3: Skin-friction coefficient of multi-shape Nanoparticles

Physical parameters			Sphere	Blade
ϕ	M	S	$-Re^{\frac{1}{2}}C_f$	
0.03	2.0	1.0	2.3045356	2.7821867
0.05	-	-	2.4928685	3.3785421
0.07	-	-	2.6859108	4.0397130
0.03	**1.5**	1.0	2.1372543	2.5816905
-	**2.0**	-	2.3045356	2.7821867
-	**2.5**	-	2.4598600	2.9683148
0.03	2.0	**1.0**	2.3045356	2.7821867
-	-	**2.0**	2.4980051	3.0139877
-	-	**3.0**	2.6784770	3.2301411

Moreover, the heat transfer rate decreases with growing values of Eckert number Ec and thermal relaxation time parameter β_1, but the opposite behavior is formed in the case of unsteadiness parameter S and Prandtl number Pr which is noted in Table 4.

Table 4: Nusselt number of multi-shape Nanoparticles

Physical parameters				Sphere	Blade
β_1	Ec	Pr	S	$Re^{-\frac{1}{2}}Nu$	
0.01	0.5	1.5	1.0	1.3525467	1.2988610
0.03	-	-	-	1.2995950	1.2506699
0.05	-	-	-	1.2473115	1.2030750
0.01	**0.5**	1.5	1.0	1.3525467	1.2988610
-	**0.7**	-	-	0.9720948	0.9345406
-	**0.9**	-	-	0.5916477	0.5702202
0.01	0.5	**1.5**	1.0	1.3525467	1.2988610
-	-	**2.0**	-	1.4595871	1.3989210
-	-	**2.5**	-	1.5405896	1.4742763
0.01	0.5	1.5	**1.0**	1.3525467	1.2988610
-	-	-	**2.0**	2.0634199	1.9755662
-	-	-	**3.0**	2.6304385	2.5151073

V. Concussion

This article studied the effect of Joule heating on the heat transfer of aluminum oxide nanofluid in the Cattaneo-Christov model over a stretched cylinder. Using BVP4C on Matlab, the relevant perspective of the proposed problem has been carried out.

- Heat transfer increases for thermal relaxation parameter, magnetic parameter, Eckert number, and volume fraction.
- Higher values of Prandtl number and unsteadiness parameter reduce the temperature profile.
- The skin friction coefficient increased for volume fraction, magnetic parameter, and unsteadiness parameter.
- The nusselt number increases for the Prandtl number and unsteadiness parameter while decreases for the Eckert number and thermal relaxation parameter.

References

[1]. M. S. Ahmed, Nanofluid: New Fluids by Nanotechnology Thermophysical Properties of Complex Materials, IntechOpen (2019).
[2]. A. Kasaeian, A. T . Eshghi and M. Sameti, A review on the applications of nanofluids flow in solar energy systems, Renewable and Sustainable Energy Reviews, 43 (2015) 584-598.
[3]. J. Fourier, The analytical theory of heat, Dover Publication, New York, (2003).
[4]. W. Ibrahim, and G. Gadisa, Finite element solution of nonlinear convective flow of Oldroyd-B fluid with Cattaneo-Christov heat flux model over nonlinear stretching surface with heat generation or absorption, Propulsion and Power Research, 9 (3) (2020) 304-315.
[5]. N. V. Ganesh, B. Ganga, A. K. A. Hakeem, S. Sarayna and R. Kalaivanan, Hydromagnetic axisymmetric slip flow along a vertical stretching cylinder with a convective boundary condition, St. Petersburg State Polytechnical University Journal; Physics and Mathematics, 4 (253) (2016) 33–47
[6]. O. D. Makine, V. Nagendramma, C. S. K. Raju, A. Leelarathna, Effects of Cattaneo-Christov heat flux on Casson nanofluid flow past a stretching cylinder, Defect and Diffusion Forum, 378 (2017) 28–38.
[7]. Babu M. Sreedhar, Thermal radiation impact and CATTANEO-CHRISTOV theory for unsteady flow of maxwell fluid over stretched cylinder with inconsistent heat source/sink, Scientific Journal, 11 (12) (2022) 1291–1311.
[8]. A. Tulu and W. Ibrahim, MHD slip flow of CNT-ethylene glycol nanofluid due to a stretchable rotating disk with Cattaneo–Christov heat flux model, Mathematical Problems in Engineering 2020 (2020) 1–13.
[9]. Z. Elahi, M. Siddiqua, A. Shahzad, Effect of Cattaneo-Christov model over a vertical stretching cylinder using SiO2 nanofluid, IJEMD-M, 2 (2023) 1-11
[10]. M. khan, A. Ahmed, M. Irfan and J. Ahmed, Analysis of Cattaneo-Christov theory for unsteady flow of Maxwell fluid over stretching cylinder, Journal of Thermal Analysis and Calorimetry, (2020) 1-10.
[11]. G. Wang, Y. Huang, Study on Joule heating effect in nanofluids. Heat and Mass Transfer, 51(4) (2015) 577-587.
[12]. S.M. Vanaki, M. Hatami, D.D. Ganji,An investigation on Joule heating effect and heat transfer in MHD nanofluids flow over a stretching sheet by means of CVFEM. Journal of Molecular Liquids, 212 (2015) 388-399.
[13]. M. Rahimi, R. Hosseini, I.Pop, Numerical simulation of nanofluid flow and heat transfer over a stretching cylinder considering the Joule heating effect. Powder Technology, 321 (2017) 358-371.

[14]. S. Han, L. Zheng, C. Li and X. Zhang, Coupled flow and heat transfer in viscoelastic fluid with Cattaneo–Christov heat flux model, Applied Mathematics Letters, 38 (2014) 87-93.
[15]. S. R. Vajjha and K. D. Debendra, Experimental determination of thermal conductivity of three nanofluids and development of new correlations, Int. J. Heat Mass Transf., 52 (21-22) (2009) 4675-4682.
[16]. R. L. Hamilton and O. K. Crosser, Thermal conductivity of heterogeneous two-component systems, Industrial & Engineering chemistry fundamentals, 1, (3), 187–191, (1962).
[17]. A. Majeed, T. Javed, and S. Shami, Numerical analysis of Walters-B fluid flow and heat transfer over a stretching cylinder, Canadian Journal of Physics, 94 (5) (2016) 522-530. 13
[18]. M. W. Maraka, M. K. Ngugi, and P. K. Roy, Similarity solution of unsteady boundary layer flow of nanofluids past a vertical plate with convective heating, Global Journal of Pure and Applied Mathematics, 14 (4) (2018) 517-534.
[19]. S. Saranya and Q. M. Al-Mdallal, Computational study on nanoparticle shape effects of Al2O3- silicon oil nanofluid flow over a radially stretching rotating disk, Case Stud.Therm. Eng., 25 (2021) 100943.
[20]. U. Hayat, S. Shaiq and A. Shahzad, A Comparative Study of Thin Film Flow of Fe3O4 and Al2O3 Nanoparticles over Stretching Surface Under the Effect of Viscous Dissipation and Magnetohydrodynamics(MHD) (2023) 10.21203/rs.3.rs-2693183/v1.
[21]. S. Shaiq, E. N. Maraj, and A. Shahzad, An unsteady instigated induced magnetic field's influence on the axisymmetric stagnation point flow of various shaped copper and silver nanomaterials submerged in ethylene glycol over an unsteady radial stretching sheet, Numerical Heat Transfer, Part A: Applications, Apr. (2023) 1–23.
[22]. E.V. Timofeeva, J. L. Routbort and D. Singh, Particle shape effects on thermophysical properties of alumina nanofluids, Journal of Applied Physics, 106 (1) (2009) 014304.
[23]. Rizwan-Ul-Haq, R. Z. H. Khan, S. T. Hussain, and Z. Hammouch; Flow and heat transfer analysis of water and ethylene glycol based Cu nanoparticles between two parallel disks with suction/injection effects, Journal of Molecular Liquids, 221 (2016) 298–304.
[24]. N.V. Ganesh, B. Ganga, A. K. A. Hakeem, S. Sarayna and R. Kalaivanan, Hydromagnetic axisymmetric slip flow along a vertical stretching cylinder with a convective boundary condition, St. Petersburg State Polytechnical University Journal. Physics and Mathematics, 4 (2016) 253.
[25]. S. M. Vanaki, H. Mohammad, A. abdollahi and M. Wahid, Effect of nanoparticle shapes on the heat transfer enhancement in a wavy channel with different phase shifts, Journal of Molecular Liquids, 196 32-42 (2014). 14